Journal of Molecular Catalysis A: Chemical 300 (2009) 111–115

Contents lists available at ScienceDirect

Journal of Molecular Catalysis A: Chemical

journal homepage: www.elsevier.com/locate/molcata

Gold-catalyzed aerobic oxidation of dibenzylamine: Homogeneous or heterogeneous catalysis?

Linda Aschwanden, Tamas Mallat, Jan-Dierk Grunwaldt[1], Frank Krumeich, Alfons Baiker*

Department of Chemistry and Applied Biosciences, ETH Hönggerberg, 8093 Zürich, Switzerland

ARTICLE INFO

Article history:
Received 2 October 2008
Received in revised form 28 October 2008
Accepted 29 October 2008
Available online 12 November 2008

Keywords:
Gold
Amine oxidation
X-ray absorption spectroscopy (XANES)
In situ spectroscopy

ABSTRACT

$Au(OAc)_3$ is applied as an effective catalyst of the selective oxidation of dibenzylamine to dibenzylimine using molecular oxygen as the only oxidant. When $Au(OAc)_3$ was preadsorbed onto CeO_2, the supported catalyst was more active than any homogeneous or heterogeneous catalyst known for this reaction. Although, some fascinating color changes in the early stage of the reaction indicated the formation of an amine complex, conventional filtration experiments proved the heterogeneity of the system. The fate of the active gold component was studied by in situ X-ray absorption spectroscopy (XANES) using a specially designed cell. These investigations revealed that in the early stage of the reaction $Au(OAc)_3$ is dissolved and subsequently reduced by the amine and the in situ formed gold nanoparticles are the real active species of the reaction. Formation of gold nanoparticles during dibenzylamine oxidation was proved independently by transmission electron microscopy. Our findings lead to a simple synthetic procedure using a commercially available gold salt, which upon interaction with the amine forms highly active and selective gold nanoparticles.

1. Introduction

Gold has received great interest in the past years as catalyst of various homogenous and heterogeneous reactions [1–4]. A milestone in the field was Haruta's work on the key importance of nanosized gold particles in low temperature CO oxidation [5]. Subsequently, gold nanoparticles were applied in various oxidation reactions including the oxidation of alcohols [6] and aldehydes [7], and the epoxidation of olefins [8]. Despite of the extensive research, it is still debated whether the active surface sites on gold nanoparticles are in metallic or cationic state during the oxidation reactions [1,9].

There are only a few reports on homogeneous catalytic oxidation reactions with gold compounds. The catalytic materials were AuCl for the oxidative cleavage of double bonds [10], Au^{III} cations generated by dissolution of Au_2O_3 for the oxidation of methane to methanol [11], $NaAuCl_4$ and $AuClPPh_3$ for the oxidation of alkanes [12], and $AuCl_2NO_3$(thioether) for thioether oxidation [13]. In most of these cases the nature of active species was not studied in detail.

Here, we report the oxidation of dibenzylamine to dibenzylimine with molecular oxygen as the only oxidant. Imines are important intermediates in organic chemistry [14,15] and their formation by the oxidation of amines has been well applied in natural product synthesis [16,17]. The best known catalysts for this reaction are Ru/Al_2O_3 [18], $Ru_2(OAc)_4Cl$ [19], Ru-hydroxyapatite [20], and CuCl [21]. Recently, even gold powder was suggested for this transformation but the turn-over frequency (TOF) was only about 0.001 h^{-1} at 100 °C [22]. From a practical point of view, gold powder cannot be considered as a catalyst, since an Au/dibenzylamine mass ratio of higher than 25 was necessary to achieve 64% conversion in 1 day. We have found that gold acetate, poorly soluble in water and organic solvents, is far more efficient in the oxidative dehydrogenation of dibenzylamine. Beside the catalytic study, we have also elucidated the probable nature of the active species by XANES.

2. Experimental

2.1. Synthesis of $Au(OAc)_3/CeO_2$

A solution of gold acetate (55.5 mg) was prepared by sonification in 300 mL deionized water at 60 °C for 2 h. The support CeO_2 (Micro Coating Technologies Inc., 2.5 g, calcined at 500 °C for 4 h, BET surface area: 117 m^2/g) was added to the vigorously stirred solution of $Au(OAc)_3$. The slurry was further shaken for 15 min, then the solid

* Corresponding author. Tel.: +41 44 632 31 53.
E-mail address: baiker@chem.ethz.ch (A. Baiker).
[1] Present address: Department of Chemical and Biochemical Engineering, Technical University of Denmark, 2800 Lyngby, Denmark.

1381-1169/$ – see front matter © 2008 Elsevier B.V. All rights reserved.
doi:10.1016/j.molcata.2008.10.049

was filtered off (the filtrate was colorless) and dried in an oven for 16 h at 80 °C. The gold content was 1.14 mass% as determined (at ALAB AG, Switzerland) by inductively coupled plasma optical emission spectrometry (ICP-OES).

2.2. Oxidation of dibenzylamine

The reaction was carried out in a 25 mL two-neck pear-shaped flask equipped with a cooler to which a balloon, connected through a three-way tap and filled with oxygen, was attached. After addition of the catalyst (60 mg), air was replaced with oxygen in the system. Through a septum, 1.5 mL of toluene was added (dried with MS 4 Å) and the stirring was turned on (750 rpm). Then 0.2 mmol dibenzylamine and an additional 1.5 mL of toluene were added. The mixture was immersed into a pre-heated oil bath. At the end of the reaction diphenylamine as internal standard was added for the GC analysis.

2.3. Characterization of the catalyst

2.3.1. In situ XANES

The experiments were performed at the ANKA-XAS beam line (Forschungszentrum Karlsruhe, Germany) using a Si(1 1 1) double crystal monochromator. An ionization chamber was used to determine the incoming X-ray intensity, the X-ray intensity behind the sample, and a third one behind gold as reference. Typically, the Si(1 1 1) crystals were slightly detuned to 70% of the incoming intensity to remove higher harmonics.

In situ XANES measurements were performed with a spectroscopic cell that allows observing the solid catalyst and the bulk liquid phase separately (Fig. 1). The technical details are described elsewhere [23]. In brief, the spectroscopic cell functions as a batch reactor that has four windows (5 mm × 1 mm) for probing with the X-ray at two positions. In the case of the experiments described in this study, the solid material is fixed in the form of a pellet at the bottom of the reactor and monitored with a path length of 4 mm through the bottom window. The bulk liquid part can be studied with a path length of 15 mm at a height of 10 mm above the bottom of the reactor cell through the upper windows. The solid and the bulk liquid phases are separated by a fine PEEK (polyetheretherketone) grid that allows the fluctuation of the reaction mixture and contact with the solid catalyst but does not allow that the solid parts enter the area where the X-ray is probing the bulk liquid. The reaction mixture is in a PEEK container that fits in the cell. The reactor is equipped with a magnetic stirrer, and a thermocouple for controlling the temperature in the cell.

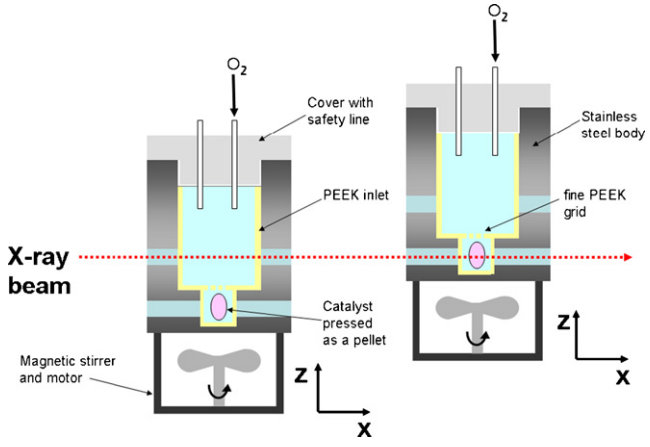

Fig. 1. Schematic presentation of the spectroscopic cell used for the in situ XANES measurements; X-ray probing the bulk liquid (left) and the solid catalyst pressed into a pellet (right). The cell was moved in *z*-direction by a home built stage with motors from Newport.

The oxidation of dibenzylamine was carried out by the following procedure. $Au(OAc)_3$ (18 mg) was mixed with Al_2O_3 (150 mg), then a pellet was pressed. From this pellet 130 mg was placed in the bottom of the spectroscopic cell. In case of studying the $Au(OAc)_3/CeO_2$ catalyst, 20 mg catalyst was mixed with Al_2O_3 (150 mg) in the pellet. From this pellet 133 mg was put into the bottom of the reactor. Once the catalyst was placed, toluene (4 mL) was added. Then the first few spectra were measured without the substrate. Subsequently, dibenzylamine (0.2 mmol) was added and the reactor was flushed with oxygen and closed. The XANES measurements were continued till the desired reaction time and temperature were reached.

The XANES data were typically recorded between 11.85 and 12.05 keV. The data were energy-corrected (first inflection point of gold foil at 11.918 keV), background-corrected, and normalized using the WINXAS 3.0 software [24]. After the $\chi(k)$ function was extracted from the XAS data, Fourier transformation was performed on the k^3-weighted data in the interval $k = 3–13.0$ Å^{-1}. Data analysis in the R-space was performed using Au–Au shells calculated by FEFF 6.0 [25]. Only the first coordination shells were used for the fittings.

2.3.2. Electron microscopy

For the TEM investigation, the catalyst was deposited onto a holey carbon foil supported on a copper grid. TEM investigations were performed with a CM30ST microscope (FEI; LaB6 cathode, operated at 300 kV, point resolution ~0.2 nm).

The particle size of the in situ formed gold nanoparticles on $Au(OAc)_3/CeO_2$ were studied with scanning transmission electron microscopy (STEM). After reaction the $Au(OAc)_3/CeO_2$ catalyst was filtered off, washed with ethyl acetate, and dried in vacuum at room temperature. The dry powder was dispersed in ethanol and deposited onto a perforated carbon foil supported on a copper grid. The investigations were performed on a Tecnai F30 microscope (FEI (Eindhoven), the field emission cathode operated at 300 kV). STEM images obtained with a high-angle annular dark field (HAADF) detector revealed Au particles with bright contrast (Z contrast). EDXS spot analysis confirmed that the bright patches corresponded to Au particles.

2.3.3. BET measurements

The specific surface area was measured using nitrogen physisorption at 77 K (−196 °C) on a Micromeritics ASAP 2000 apparatus. The 5-point BET method was applied in the range $0.05 < p/p_0 < 0.25$. All samples were degassed at 100 °C for several hours before the measurements.

3. Results and discussion

3.1. Oxidation of dibenzylamine

The oxidation of dibenzylamine with oxygen was investigated in toluene under atmospheric pressure. The activity of $Au(OAc)_3$ and the selectivity to dibenzylimine improved with increasing temperature (Table 1). Above 80 °C the conversion barely changed, due to the decreasing solubility of oxygen in toluene at close to the reflux temperature (entries 2–4). The major byproduct was benzaldehyde and a small amount of benzonitrile and benzylamine (<0.5%) was also formed. Formation of these is initiated by the hydrolysis of the imine [26]. Hence, the improved selectivity at higher reaction temperatures may simply be attributed to the removal of water by-product of amine oxidation from the reaction mixture.

Table 1
Aerobic oxidation of dibenzylamine[a].

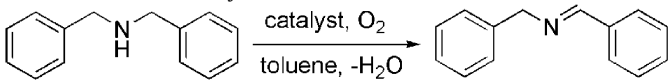

.

Entry	Catalyst	Time [h]	Temp. [°C]	Conversion [%]	Selectivity [%]	TOF[b] [h^{-1}]
1	$Au(OAc)_3$[c]	24	r. t.	15	76	0.02
2	$Au(OAc)_3$[c]	7.15	81	93	94	0.54
3	$Au(OAc)_3$[c]	7.15	91	96	95	0.56
4	$Au(OAc)_3$[c]	7.15	108	100	97	0.58
5	$Au(OAc)_3$[c]	4	108	94	96	0.98
6	$Au(OAc)_3/CeO_2$[d]	8	108	99.7	91	7.2
7	CeO_2[e]	24	91	0	0	0
8	No catalyst	24	91	0	0	0

[a] 60 mg catalyst, 0.2 mmol dibenzylamine, 3 mL toluene, 1 bar O_2.
[b] Related to the total amount of Au.
[c] 24.1 mol% related to the amine.
[d] 1.7 mol% Au related to the amine.
[e] 60 mg ceria.

The reaction rate could be enhanced remarkably by adsorbing gold acetate from a dilute aqueous solution onto ceria and using the dried, supported salt for oxidation. In the best case the average TOF was 7.2 h^{-1} at 99.7% conversion (Table 1, entry 6) or 9.2 h^{-1} at 80% conversion of dibenzylamine (not shown). For comparison, the most efficient catalysts of dibenzylamine oxidation, mentioned in the introduction, afforded TOFs of 0.2–3.8 h^{-1} and the selectivities to the imine were in the range 74–93% [18–21,27]. The last two entries in Table 1 show that ceria was completely inactive and no background oxidation could be detected.

3.2. Heterogeneity test

Gold acetate is a black powder that is insoluble in toluene. When the amine was added to the slurry at room temperature, the liquid phase became reddish and then brown, indicating a possible dissolution of the catalyst as an amine complex. Later, by heating the slurry to the reaction temperature, the color gradually turned to dark purple and then black. In a leaching test, the reaction catalyzed by $Au(OAc)_3$ at 91 °C was stopped after 3 h at 60% conversion and the solid phase was filtered off. The oxidation was continued with the filtrate for 3 h but the conversion did not change.

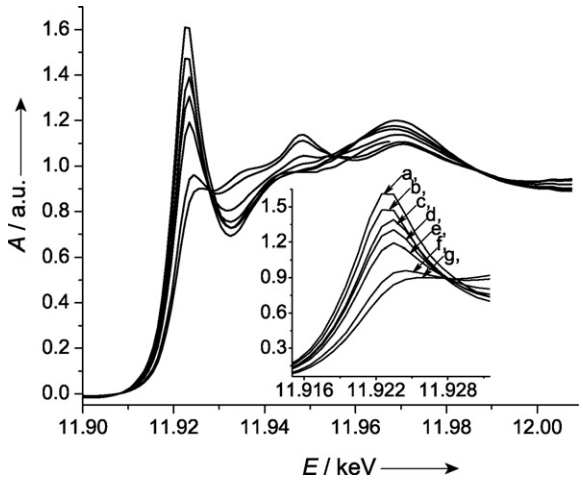

Fig. 2. XANES spectra of gold during the oxidation of dibenzylamine with $Au(OAc)_3$ (bottom window of the cell, solid phase); (a) room temperature (r. t.) without stirring (b), r. t. with stirring, (c) r. t. after addition of the amine, (d) 60 °C, (e) 64 °C, (f) 91 °C, (g) 91 °C (20 min later).

For testing the heterogeneity of $Au(OAc)_3/CeO_2$, the reaction carried out at 108 °C was stopped after 1.5 h, at 39% conversion. The reaction mixture was filtered over two layers of a very fine filter (Whatman Glass Microfibre Filter GF/D; between the layers 2 g Celite was packed). After separation, the reaction was continued with the filtrate under the same reaction conditions for another 6 h but the conversion did not change.

3.3. Nature of the active site determined by XANES

To clarify the nature of the active species, we used in situ XANES. This technique can be well applied to investigate the characteristics of the active sites, including the oxidation state under reaction conditions [28–32]. Our special spectroscopic cell [23] allowed following the changes in a two-phase system (Fig. 1). When the X-ray was led through the bottom window of the cell the changes in the catalyst (pressed as a pellet with Al_2O_3 diluent) were monitored, whereas through the upper window the changes in the liquid phase were studied.

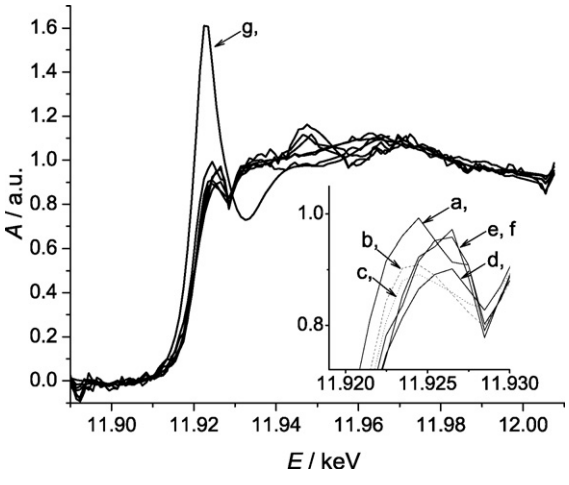

Fig. 3. XANES spectra of gold during the oxidation of dibenzylamine with $Au(OAc)_3$ (upper window of the cell, liquid phase); (a) r. t. after addition of the amine, (b) r. t. (10 min later), (c) 46 °C, (d) 87 °C, (e) 91 °C, (f) 91 °C (20 min later); (g) $Au(OAc)_3$ in the solid phase (pellet) at r. t. before addition of the amine (as reference, the same as Fig. 2a).

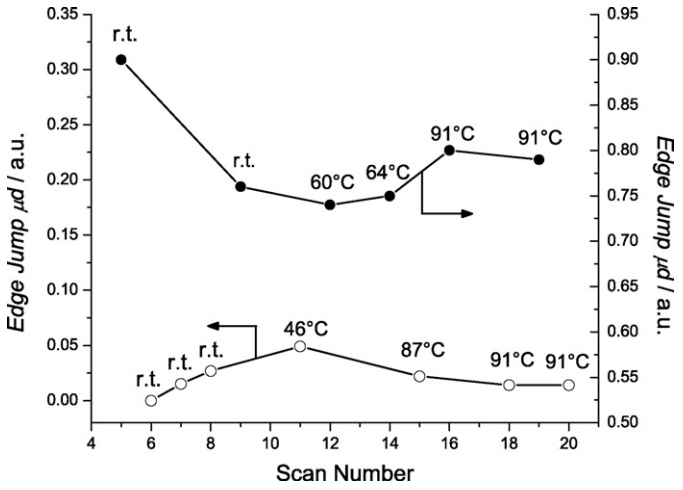

Fig. 4. Edge jump of the XANES data of gold during the oxidation of dibenzylamine with $Au(OAc)_3$ solid phase (bottom window of the cell, ●) and liquid phase (upper window of the cell, ○). The edge jump is proportional to the amount of gold.

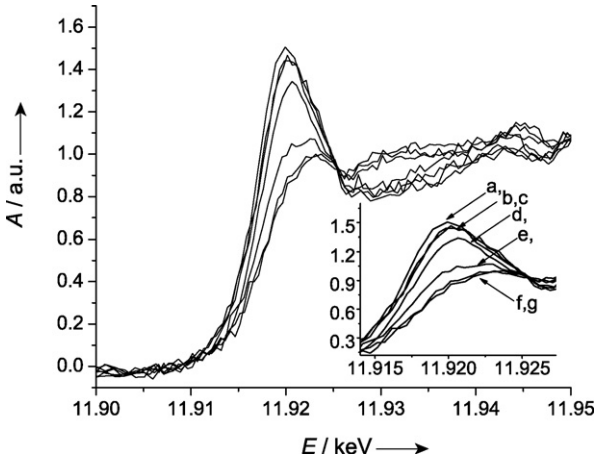

Fig. 5. XANES spectra of gold during the oxidation of dibenzylamine with $Au(OAc)_3/CeO_2$ (bottom window of the cell, solid phase); (a) r. t. without stirring, (b) r. t. with stirring, (c) r. t. after addition of the amine, (d) 59 °C, (e) 59 °C, (f) 91 °C, (g) 91 °C.

3.3.1. $Au(OAc)_3$ pellet as the catalyst of dibenzylamine oxidation

At first, we simulated the early stage of amine oxidation and followed the oxidation state of gold in the pellet prepared from $Au(OAc)_3$. The decrease in the white line in Fig. 2 reveals that gold was reduced to the metallic state at the reaction temperature of 91 °C.

The XANES spectra collected in the upper part of the cell during the same experiment are presented in Fig. 3. There was no detectable gold in toluene before addition of dibenzylamine, in agreement with the insolubility of $Au(OAc)_3$. After addition of the amine, gold appeared in the liquid phase (Fig. 3a) mainly in a reduced state. The spectrum of untreated $Au(OAc)_3$ in the solid phase is depicted for comparison (Fig. 3g). A further reduction of the leached gold continued till a medium temperature was reached (Fig. 3a–c) and then the average oxidation state of gold slightly increased again (Fig. 3d–f). Based on the changes of the edge jump of the XANES of the liquid phase (Fig. 4, ○), the amount of leached gold species in solution increased until a medium temperature (ca. 46–60 °C) was reached and then decreased again till the end of the experiment. Meanwhile, in the solid phase (Fig. 4, ●) the amount of gold decreased till 60 °C then increased again. (*Note* that some uncertainty in the mass balance was caused by deposition of a small amount of gold which precipitated on the wall of the in situ cell. However, this observation does not change the general tendency shown in Fig. 4.) From these observations it can be assumed that the amine coordinates to $Au(OAc)_3$ that is in the pellet and takes the gold into solution, but this complex is rapidly reduced to metallic gold. At above 60 °C the gold from the liquid phase starts to deposit onto the catalyst pellet, which explains the increasing amount of Au in the solid phase during this period (Fig. 4, ●). Since metallic gold is steadily removed from the liquid, a slight increase in the average oxidation state of gold in solution is observed at higher temperatures (Fig. 3d–f).

Comparison of the XANES data and the results of the filtration experiments of the unsupported $Au(OAc)_3$ catalyst suggests that the trace amount of cationic gold, detected by XANES in the liquid phase, is probably a spectator as it cannot convert dibenzylamine. An alternative and more probable explanation is that the cationic gold is present on the surface of metallic gold particles and removed from solution by filtration. In this case the contribution of ionic

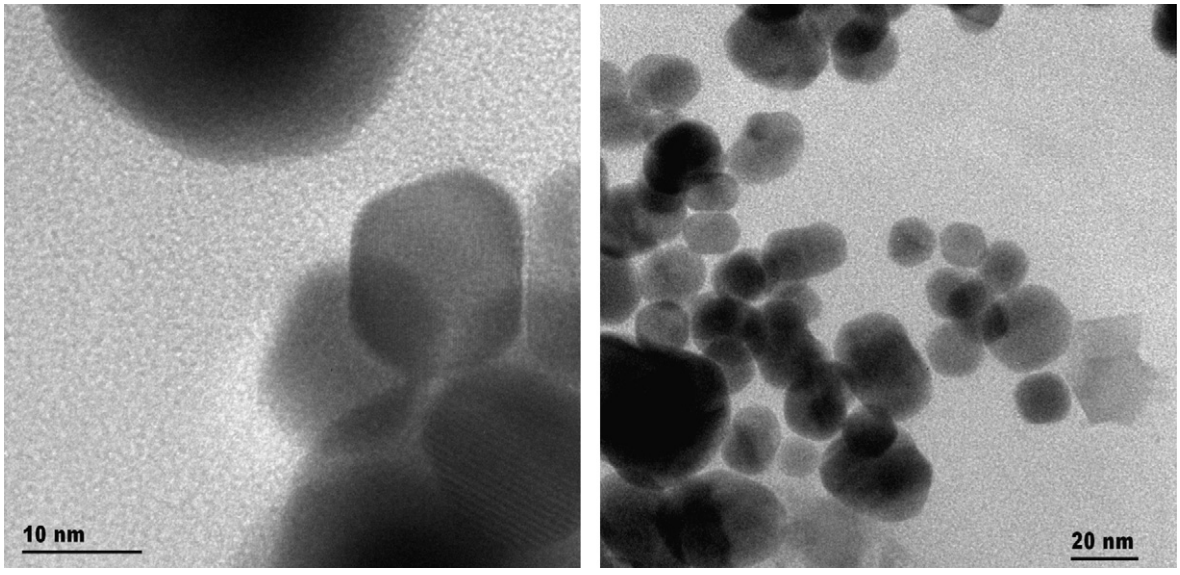

Fig. 6. TEM image of gold nanoparticles formed in situ from $Au(OAc)_3$ during the oxidation of dibenzylamine.

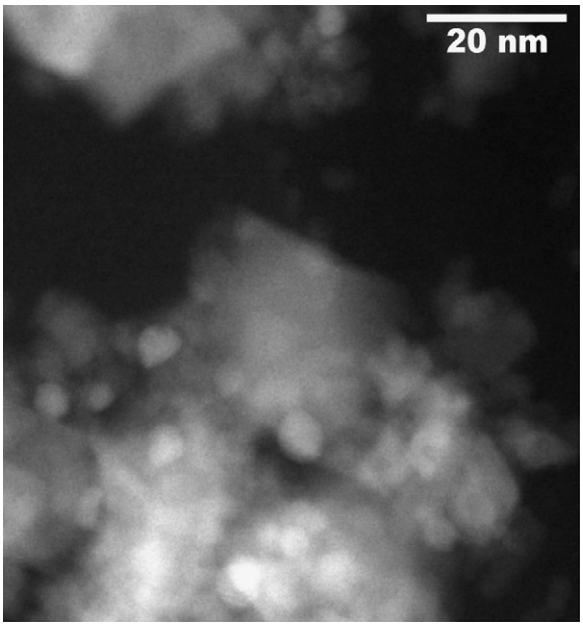

Fig. 7. Gold nanoparticles formed in situ when using $Au(OAc)_3/CeO_2$ for amine oxidation (imaged by Z-contrast STEM).

gold species to amine oxidation cannot be ruled out, although the amount of ionic species and their possible contribution seems to be negligible.

3.3.2. $Au(OAc)_3/CeO_2$ pellet as the catalyst of dibenzylamine oxidation

Next we used $Au(OAc)_3/CeO_2$ (1.14 mass% Au) to catalyze the oxidation of dibenzylamine in the reactor cell (Fig. 5.). The spectra were taken through the bottom window of the cell. The results are very similar to those presented in Fig. 2: the average oxidation state of gold decreased with time and increasing temperature and gold was fully reduced by the time the reaction temperature of 91 °C was reached. A major difference to the experiment with unsupported $Au(OAc)_3$ was that in this case no traces of gold were detected in the liquid phase, indicating a strong interaction between gold and ceria.

3.4. Electron microscopic study

Formation of gold nanoparticles during dibenzylamine oxidation was proved independently by electron microscopy. After amine oxidation with unsupported $Au(OAc)_3$ the powder was filtered off and analyzed with TEM (Fig. 6). The Au particle size was in the range 10–50 nm and the particles were partially agglomerated. The crystalline characteristic of gold nanoparticles is shown by the presence of lattice fringes. The measured lattice spacing of 0.23 nm corresponds well to the (1 1 1) plane of Au (theoretical value: 0.235 nm).

Due to the support effect, the gold nanoparticles formed in situ from the $Au(OAc)_3/CeO_2$ were much smaller, in the range 5–10 nm, and no agglomeration was observed by STEM (Fig. 7).

4. Conclusions

In conclusion, we found that $Au(OAc)_3$ can be used as an efficient catalyst for the selective oxidation of dibenzylamine to dibenzylimine with molecular oxygen as the only oxidant. XANES combined with TEM revealed that in the early stage of the reaction $Au(OAc)_3$ is dissolved and subsequently reduced, and the in situ formed gold nanoparticles catalyze the reaction.

Acknowledgements

We thank ANKA (Forschungszentrum Karlsruhe) for providing beamtime and the European Community (Integrated Infrastructure Initiative 'Integrating Activity on Synchrotron and Free Electron Laser Science', Contract RII3-CT-2004-506008) and ETH Zürich for financial support. EMEZ (electron microscopy ETH Zurich) is acknowledged for microscope time. We thank Bertram Kimmerle and Björn Schimmöller for their help in catalyst characterization.

References

[1] A.S.K. Hashmi, G.J. Hutchings, Angew. Chem. Int. Ed. Engl. 45 (2006) 7896.
[2] S. Demirel-Gulen, M. Lucas, P. Claus, Catal. Today 102 (2005) 166.
[3] M. Haruta, M. Daté, Appl. Catal. A 222 (2001) 427.
[4] G.C. Bond, D.T. Thompson, Catal. Rev. Sci. Eng. 41 (1999) 319.
[5] M. Haruta, N. Yamada, T. Kobayashi, S. Iijima, J. Catal. 115 (1989) 301.
[6] T. Mallat, A. Baiker, Chem. Rev. 104 (2004) 3037.
[7] S. Biella, L. Prati, M. Rossi, J. Mol. Catal. A: Chem. 197 (2003) 207.
[8] A.K. Sinha, S. Seelan, S. Tsubota, M. Haruta, Angew. Chem. Int. Ed. Engl. 43 (2004) 1546.
[9] Q. Fu, H. Saltsburg, M. Flytzani-Stephanopoulos, Science 301 (2003) 935.
[10] D. Xing, B.T. Guan, G.X. Cai, Z. Fang, L.P. Yang, Z.J. Shi, Org. Lett. 8 (2006) 693.
[11] C.J. Jones, D. Taube, V.R. Ziatdinov, R.A. Periana, R.J. Nielsen, J. Oxgaard, W.A. Goddard, Angew. Chem. Int. Ed. Engl. 43 (2004) 4626.
[12] G.B. Shul'pin, A.E. Shilov, G. Süss-Fink, Tetrahedron Lett. 42 (2001) 7253.
[13] E. Boring, Y.V. Geletii, C.L. Hill, J. Am. Chem. Soc. 123 (2001) 1625.
[14] J.S.M. Samec, A.H. Éll, J.E. Bäckvall, Chem. Eur. J. 11 (2005) 2327.
[15] S.I. Murahashi, Angew. Chem. Int. Ed. Engl. 34 (1995) 2443.
[16] G.A. Kraus, A. Melekhov, Tetrahedron 54 (1998) 11749.
[17] Y. Jinbo, H. Kondo, M. Taguchi, F. Sakamoto, G. Tsukamoto, J. Org. Chem. 59 (1994) 6057.
[18] K. Yamaguchi, N. Mizuno, Angew. Chem. Int. Ed. Engl. 42 (2003) 1480.
[19] S.I. Murahashi, Y. Okano, H. Sato, T. Nakae, N. Komiya, Synlett (2007) 1675.
[20] K. Mori, K. Yamaguchi, T. Mizugaki, K. Ebitani, K. Kaneda, Chem. Commun. (2001) 461.
[21] Y. Maeda, T. Nishimura, S. Uemura, Bull. Chem. Soc. Jpn. 76 (2003) 2399.
[22] B.L. Zhu, R.J. Angelici, Chem. Commun. (2007) 2157.
[23] J.D. Grunwaldt, M. Ramin, M. Rohr, A. Michailovski, G.R. Patzke, A. Baiker, Rev. Sci. Instrum. 76 (2005) 054104.
[24] T. Ressler, J. Synchrotron Radiat. 5 (1998) 118.
[25] S.I. Zabinsky, J.J. Rehr, A. Ankudinov, R.C. Albers, M.J. Eller, Phys. Rev. B 52 (1995) 2995.
[26] T. Mallat, A. Baiker, W. Kleist, K. Köhler, in: G. Ertl, H. Knözinger, F. Schüth, J. Weitkamp (Eds.), Handbook of Heterogeneous Catalysis, Wiley–VCH, Weinheim, 2008, pp. 3548–3564.
[27] A.J. Bailey, B.R. James, Chem. Commun. (1996) 2343.
[28] D. Bazin, H. Dexpert, J. Lynch, X-ray Absorption Fine Structure For Catalysts and Surfaces, World Scientific, Singapore, 1996.
[29] M.K. Schröter, L. Khodeir, M.W.E. van den Berg, T. Hikov, M. Cokoja, S.J. Miao, W. Grünert, M. Muhler, R.A. Fischer, Chem. Commun. (2006) 2498.
[30] P. Haider, J.D. Grunwaldt, R. Seidel, A. Baiker, J. Catal. 250 (2007) 313.
[31] S.R. Bare, G.E. Mickelson, F.S. Modica, A.Z. Ringwelski, N. Yang, Rev. Sci. Instrum. 77 (2006) 023105.
[32] A.I. Frenkel, S. Nemzer, I. Pister, L. Soussan, T. Harris, Y. Sun, M.H. Rafailovich, J. Chem. Phys. 123 (2005) 184701.